

Supporting Information

Structure elucidation of multicolor emissive graphene quantum dots towards cell guidance

I. Jénnifer Gómez,^{*a} Manuel Vázquez Sulleiro,^b Anna Dolečková,^c Naděžda Pizúrová,^d Jiřina Medalová,^c Antonín Bednařík,^e Jan Preisler,^e David Nečas,^f Lenka Zajíčková^{*a,f}

^a Department of Condensed Matter Physics, Faculty of Science, Masaryk University, Kotlářská 2, 611 37 Brno, Czech Republic

^b IMDEA Nanociencia, Faraday 9, 280 49 Ciudad Universitaria de Cantoblanco Madrid, Spain

^c Department of Experimental Biology, Faculty of Science, Masaryk University, Kamenice 5, 625 00 Brno, Czech Republic

^d Institute of Physics of Materials, Žitkova 22, 616 62 Brno, Czech Republic

^e Department of Chemistry, Faculty of Science, Masaryk University, Kamenice 5, 625 00 Brno, Czech Republic

^f Central European Institute of Technology - CEITEC Brno University of Technology, Purkyňova 123, 612 00 Brno, Czech Republic

Table of Contents

1. Reagents and materials.....	2
2. Synthesis photographs.....	2
3. MALDI MS measurements.....	3
4. AFM measurements.....	6
5. TEM measurements.....	6
6. Kaiser test.....	7
7 XPS measurements.....	8
8. NMR measurements.....	9
9. TGA measurements.....	13
10. Raman measurements.....	14
11. XRD measurements.....	15
12. Fluorescence measurements.....	15
13. Cell stability.....	17
14. Cell viability.....	17
15. Confocal laser scanning microscope control images.....	18
16. References.....	19

1. Reagent and materials

Glucose, ammonium hydroxide and Kaiser test kit were purchased from Sigma-Aldrich, USA. All the reagents were used as supplied without further purifications. Dialysis membrane tubes with a cut-off 0.5-1 kDa were supplied by Spectrum Labs, USA. Ultrapure water used in all the experiments was produced using a Milli-Q water system (Millipore, Merck, Germany). Human vascular smooth muscle cells (VSMC) were isolated at Laboratory of Biomaterials and Tissue Engineering, Institute of Physiology, Czech Academy of Science. Dulbecco's modified Eagle's medium (DMEM), high glucose, fetal bovine serum (FBS) and L-glutamine were purchased from Gibco, Thermo Fisher Scientific, USA. Penicillin/Streptomycin was supplied by HyClone, Thermo Fisher Scientific. ATP release reagent was produced by Sigma Aldrich, and was used to quantify relative cell viability. 1 x Trypsin-Ethylene-diamine tetraacetic acid (Trypsin-EDTA) was obtained from Biotech, Sweden and DRAQ5 nuclear stain was purchased from Cell Signaling Technology, USA. 8 Chambered Coverglass System was purchased from CellVis, USA. Microtiter white 96 well flat bottom strips were acquired from Thermo Fisher Scientific and luciferase/luciferin mixture from BioThema, Sweden.

2. Synthesis photographs

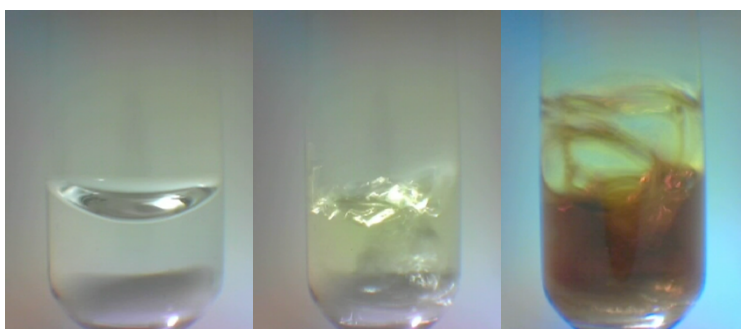


Figure S1. Photographs of the microwave hydrothermal method along the reaction time.

3. MALDI MS measurements

MALDI TOF MS spectra were recorded at m/z range 0 – 5000 and 0 – 2000 for linear and reflector mode, respectively; ions with m/z up to 100 Da were deflected. Together, 1000 shots were accumulated per spectrum at the laser energy level of 85%. In the linear mode, the voltages Ion Source 1 and Ion Source 2 were set to 19.50 and 18.35 kV, respectively. The lens voltage was 6.00 kV and the time of pulsed ion extraction was 130 ns. In the reflector mode, the voltages Ion Source 1 and Ion Source 2 were set to 19.50 and 18.35 kV, respectively. The lens voltage was 6.00 kV and the time of pulsed ion extraction was 130 ns.

SubAP-MALDI MS spectra obtained using the orbital trapping instrument were recorded using laser (355 nm, 1000Hz) scanning the samples at the constant speed raster motion (CSR) mode at speed 3.445 mm/min. Resolving power was set to 280000 at $m/z = 200$, injection time (IT) was 1000 ms. Voltages V_7 - V_1 applied across the MALDI target and ion funnel electrodes ensuring efficient transfer of the generated ions into the mass spectrometer were 350, 250, 150, 120, 90, 85, and 30 V, respectively; the radiofrequency (RF) amplitude was 130 V (peak-to-peak).

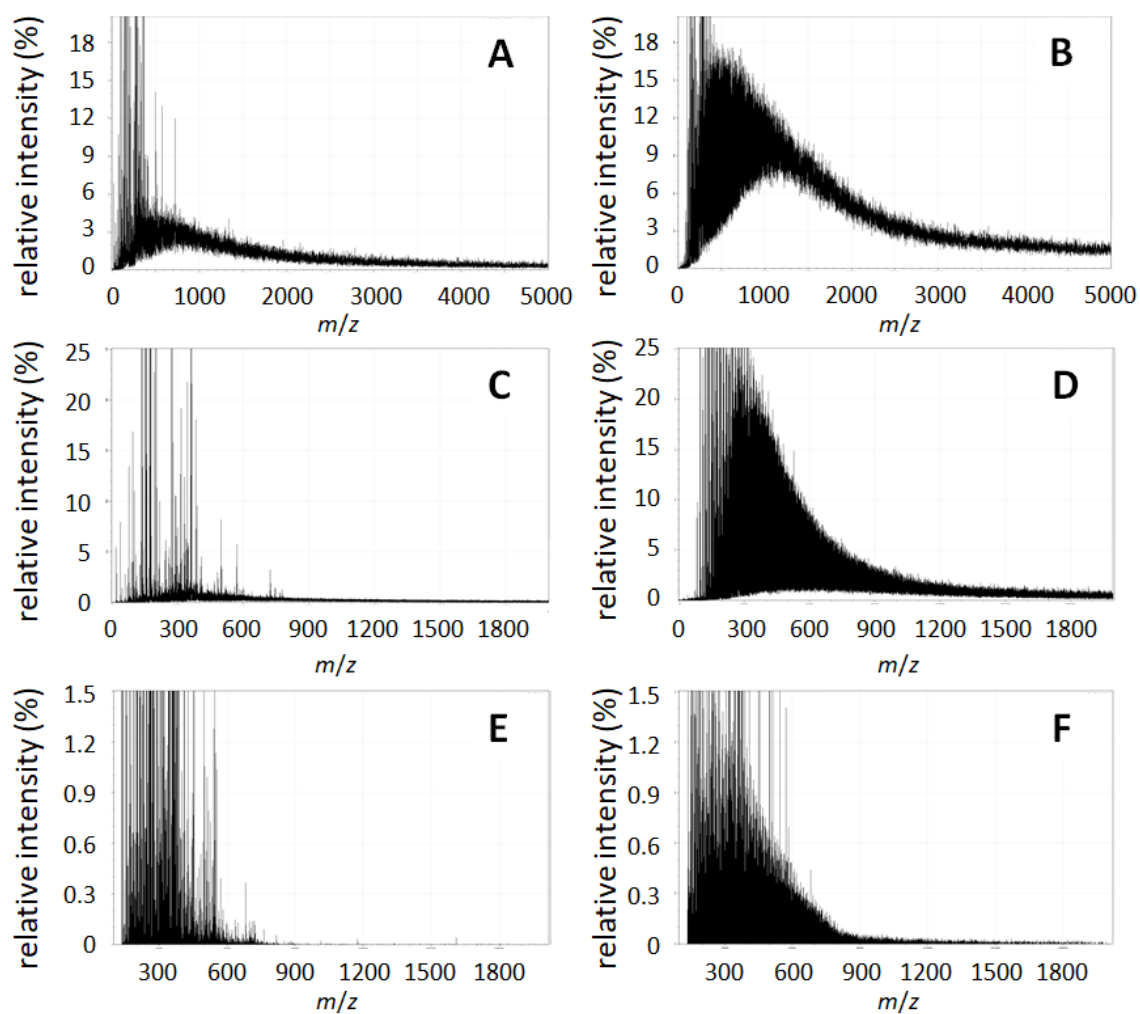


Figure S2. MALDI mass spectra of reaction mixtures at T0 (A,C,E) and T4 (B,D,F) recorded with A, B) linear TOF MS; C, D) reflector TOF MS and E,F) subAP-MALDI orbital trapping MS

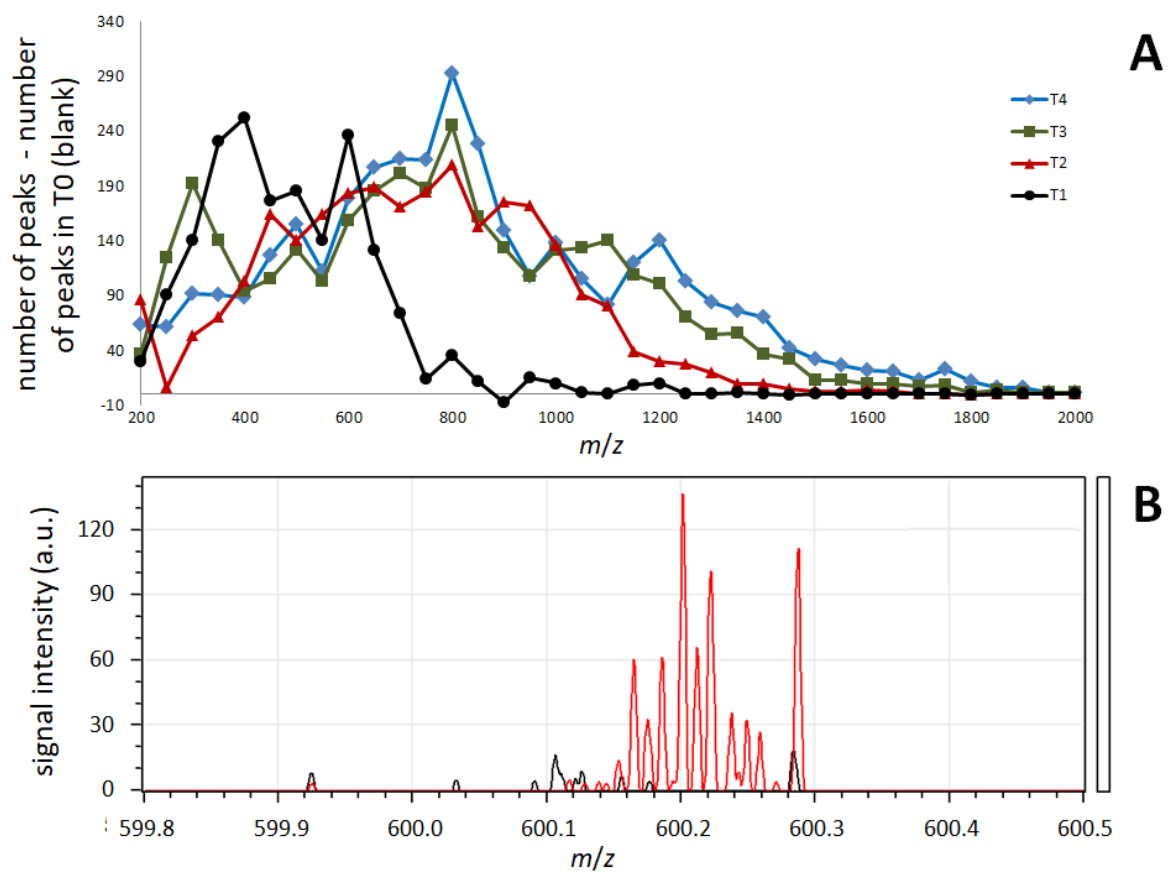


Figure S3. A) The total number of peaks at 50 Da wide bins observed using the ultra-high resolution subAP-MALDI MS. Number of peaks at the same 50 Da wide bins of T0 blank sample was subtracted. B) Zoom at m/z 600 showing new peaks observed after reaction (T0 – black, T4 – red).

4. AFM measurements

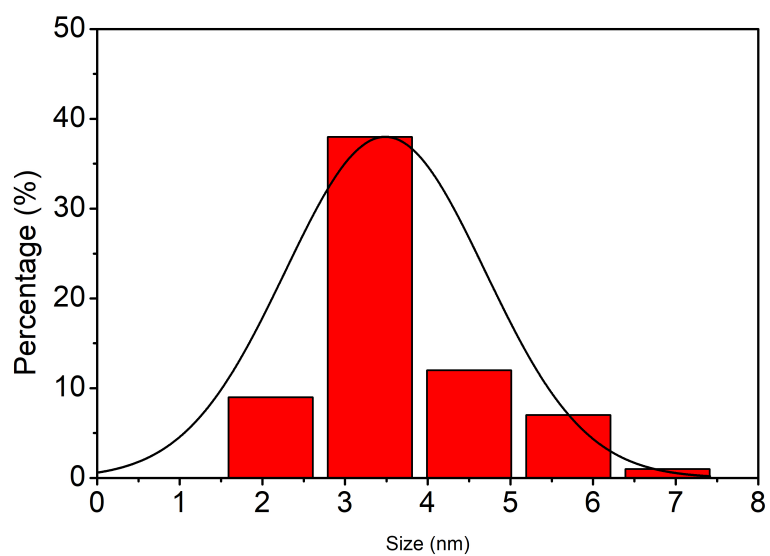


Figure S4. Size distribution histogram of GQDs.

5. TEM measurements

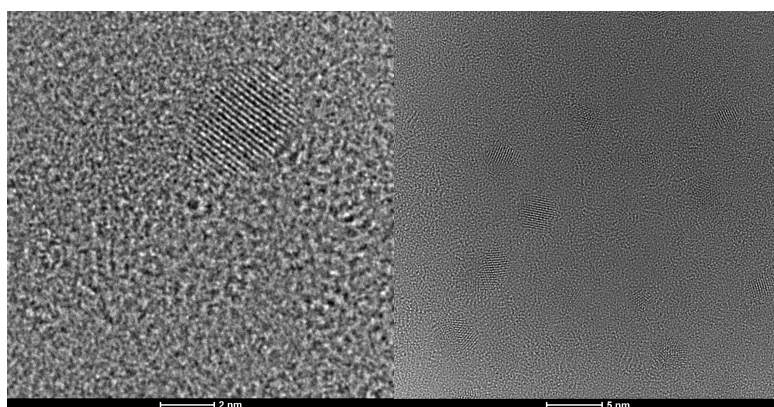
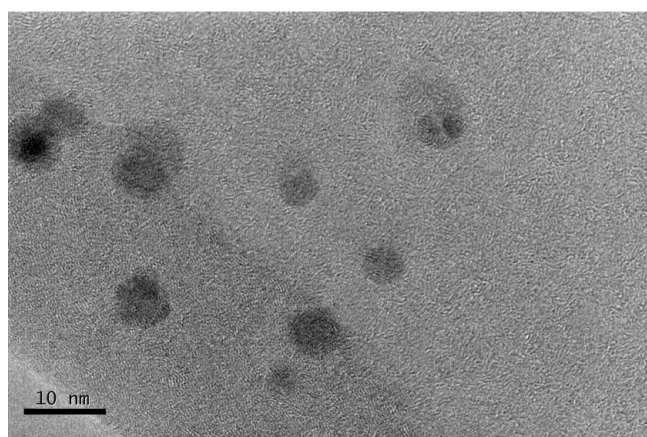


Figure S5. TEM and HRTEM images of GQDs.

6. Kaiser test

The free amino groups of the GQDs were determined by so-called Kaiser test,⁴ using a commercial kit. The Kaiser test is based on the intense blue color generated by the reaction of ninhydrin with free primary amines, which is then measured spectrophotometrically. First, 0.5 mg of GQDs were weighed, then the following solution reagents were added: 75 μL of solution 1 (80 g of phenol in 20 mL of ethanol), 100 μL of solution of 2 (2 mL of KCN 1 mM in water in 98 mL of pyridine), and 75 μL of solution 3 (1 g of ninhydrin in 20 mL of ethanol). The mixture was heated at 120 $^{\circ}\text{C}$ for 10 min and finally diluted with ethanol 60 % up to a final volume of 3 mL. For the quantitative determination of the free amino groups on the surface of the dots, the absorbance was recorded at 570 nm, setting the zero on the blank without sample. The ratio between the moles of the primary amines moiety and the weight of the sample is given by:

$$[NH_2] = \frac{A_{570} \cdot V}{\epsilon \cdot m} \quad (1)$$

where A_{570} is the absorbance at 570 nm, V the final volume after dilution (3 mL), ϵ is the molar extinction coefficient ($15000 \text{ M}^{-1}\text{cm}^{-1}$), m is the mass of N-GQDs.

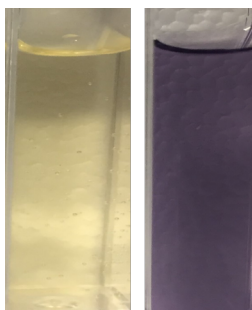


Figure S6. Photograph of the positive Kaiser test of GQDs. Right violet colour generated by the reaction of ninhydrin, left the yellow colour of the reference.

7. XPS measurements

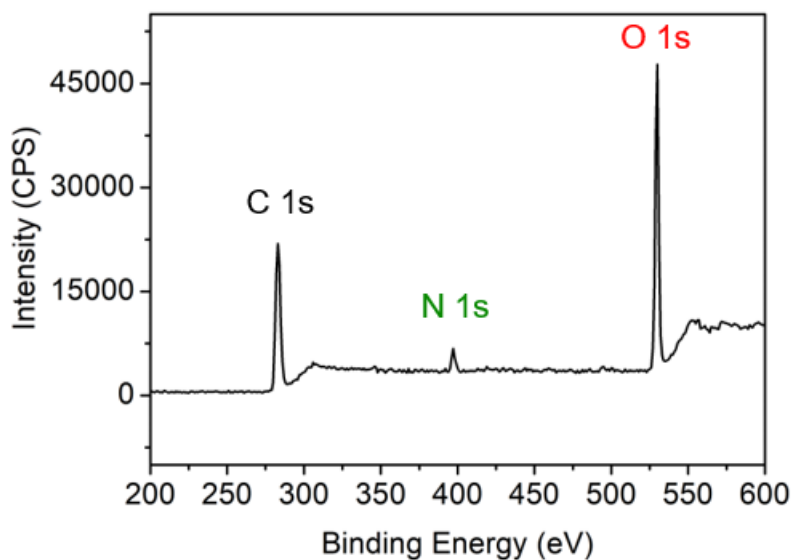


Figure S7. XPS survey of GQDs.

Table S1. Binding energy and percentage of C, N, and O atoms in GQDs as determined by XPS measurements.

Core Level	Binding Energy (eV)	Atomic composition (%)
C 1s	286.0	64.6
C-C/C=C	284.5	36.4
C-O/C-N	286.1	48.4
C=O/C=N	287.7	13.7
COOH	289.1	1.4
N 1s	399.5	3.5
N=C/NH ₂	399.4	88.6
N-C ₃	401.5	11.4
O 1s	531.0	31.9
O=C	529.4	15.0
O-C	531.0	82.5
C-O-C	533.6	2.5

8. NMR measurements

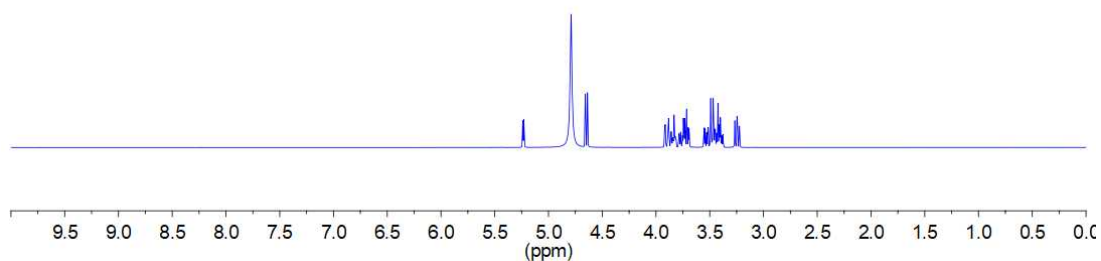


Figure S8. ^1H NMR spectra of glucose in D_2O .

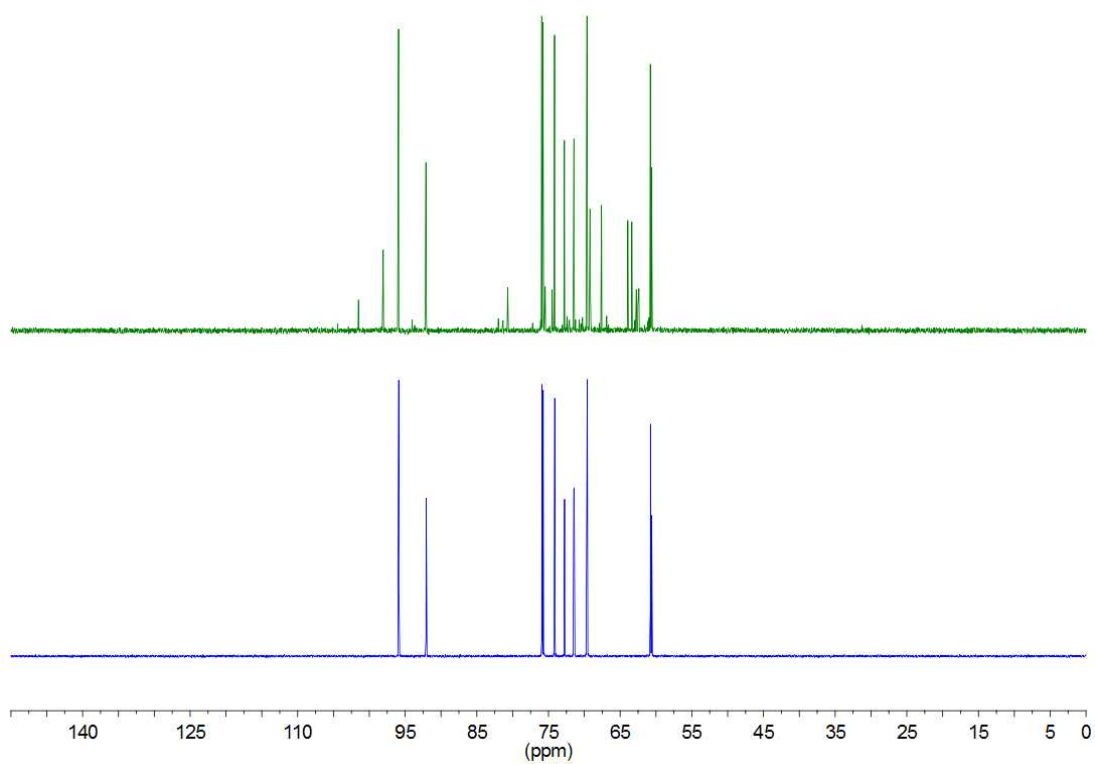


Figure S9. ^{13}C NMR spectra GQDs (green) and glucose (blue). All the experiments were recorded with D_2O .

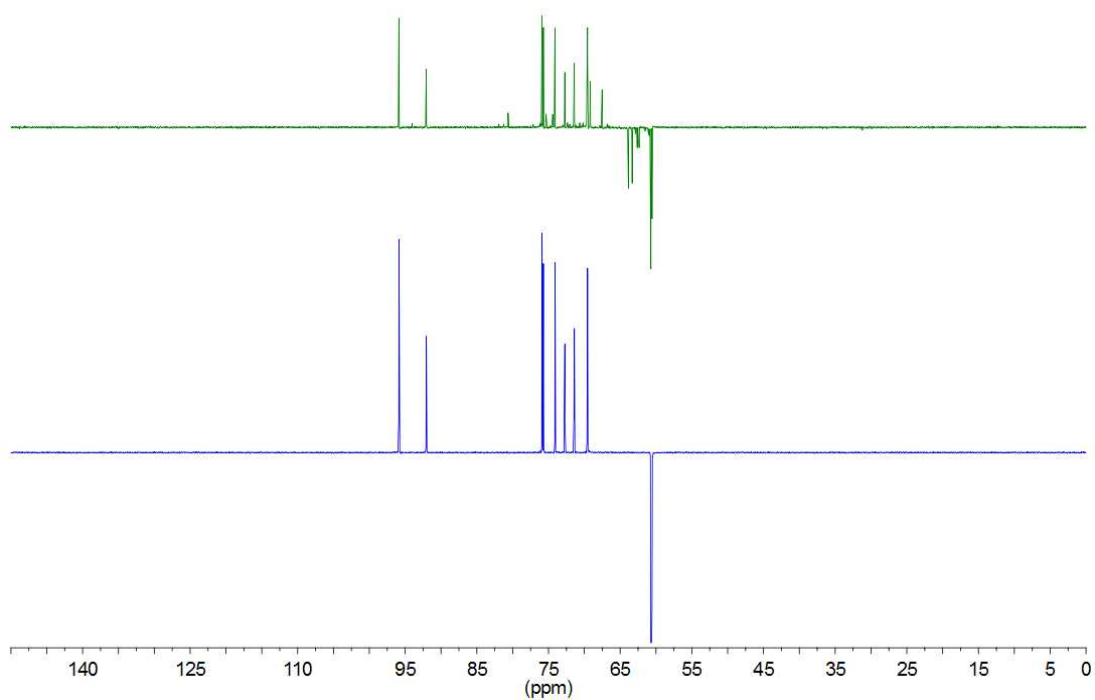


Figure S10. ¹³C DEPT 135 NMR spectra GQDs (green) and glucose (blue). All the experiments were recorded with D₂O.

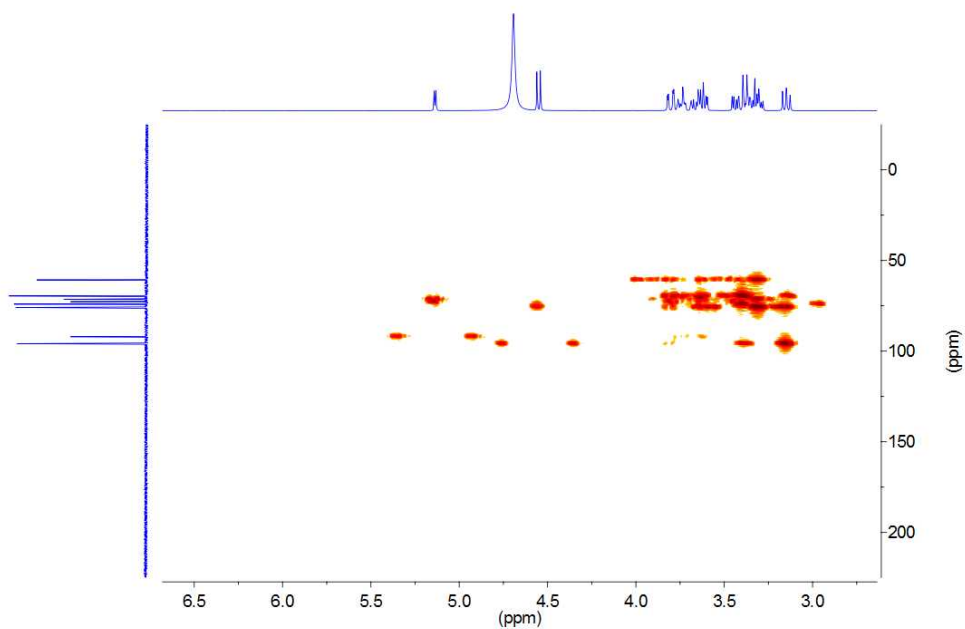


Figure S11. HMBC spectrum of glucose in D₂O.

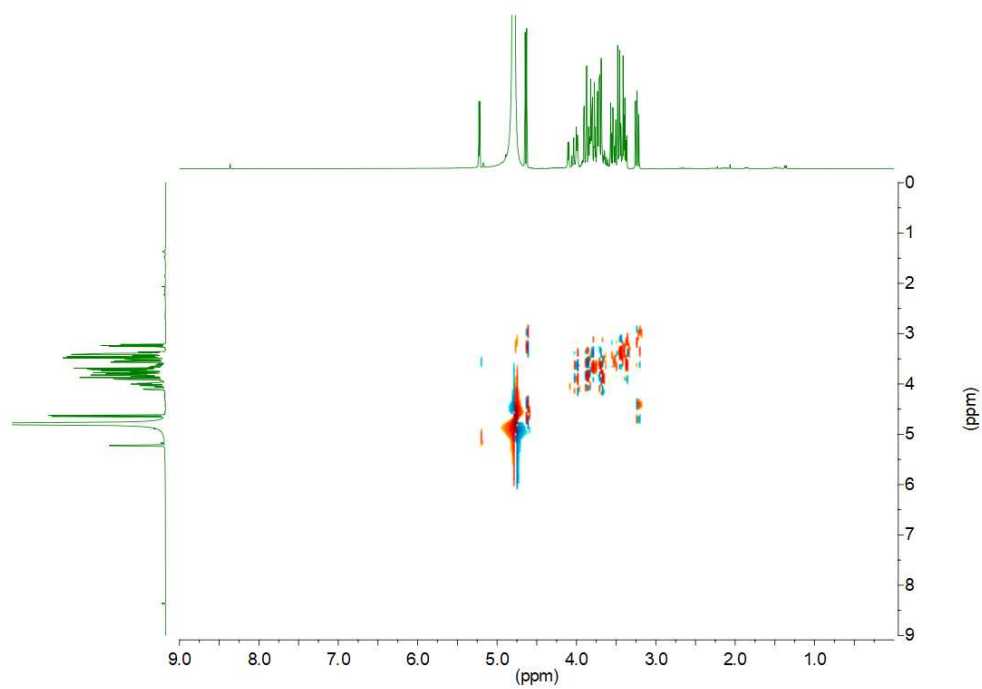


Figure S12. COSY spectrum of GQDs in D₂O.

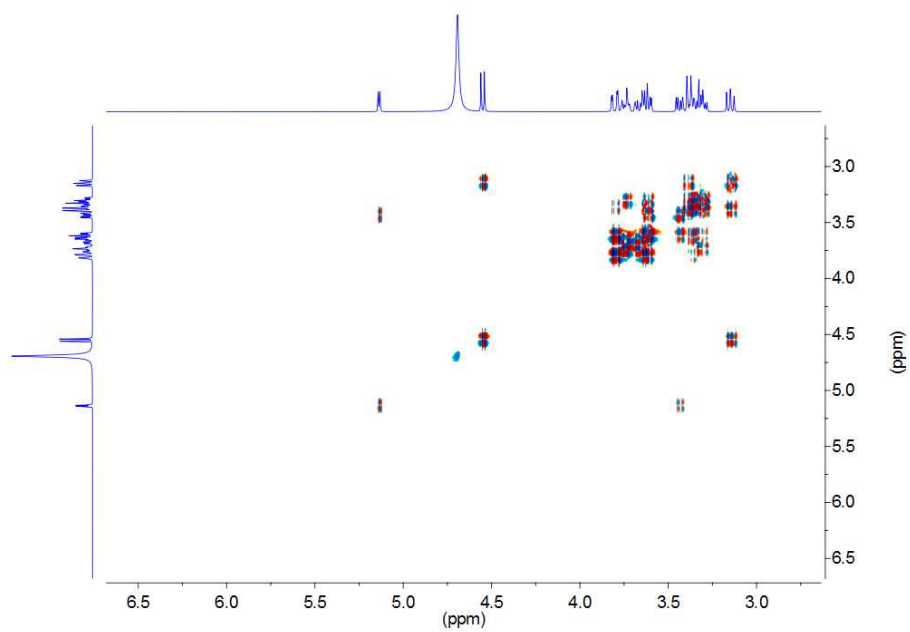


Figure S13. COSY spectrum of glucose in D₂O.

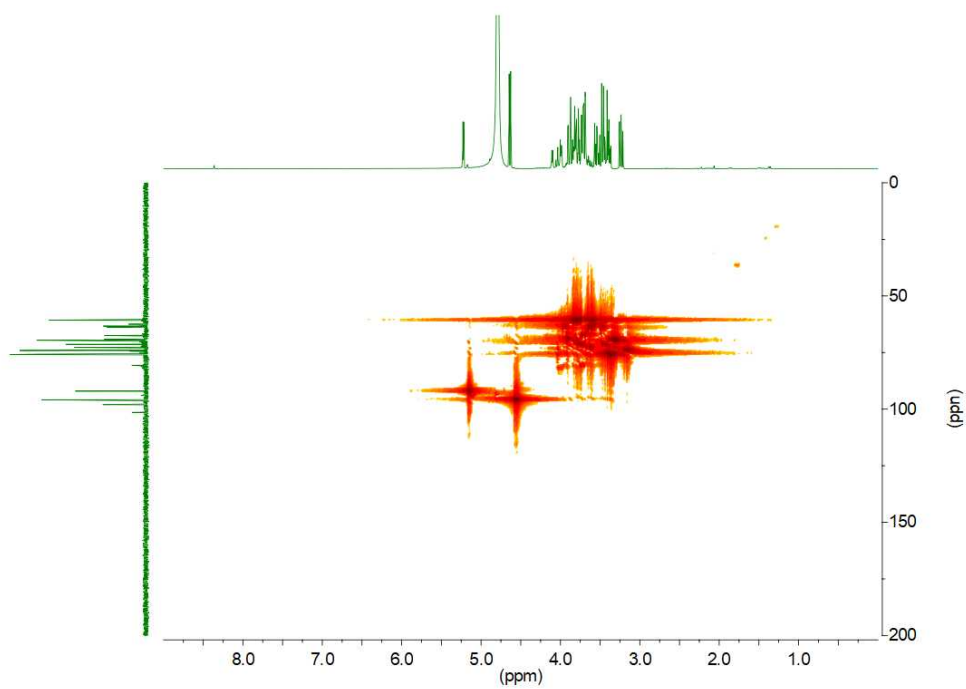


Figure S14. HMQC spectrum of GQDs in D₂O.

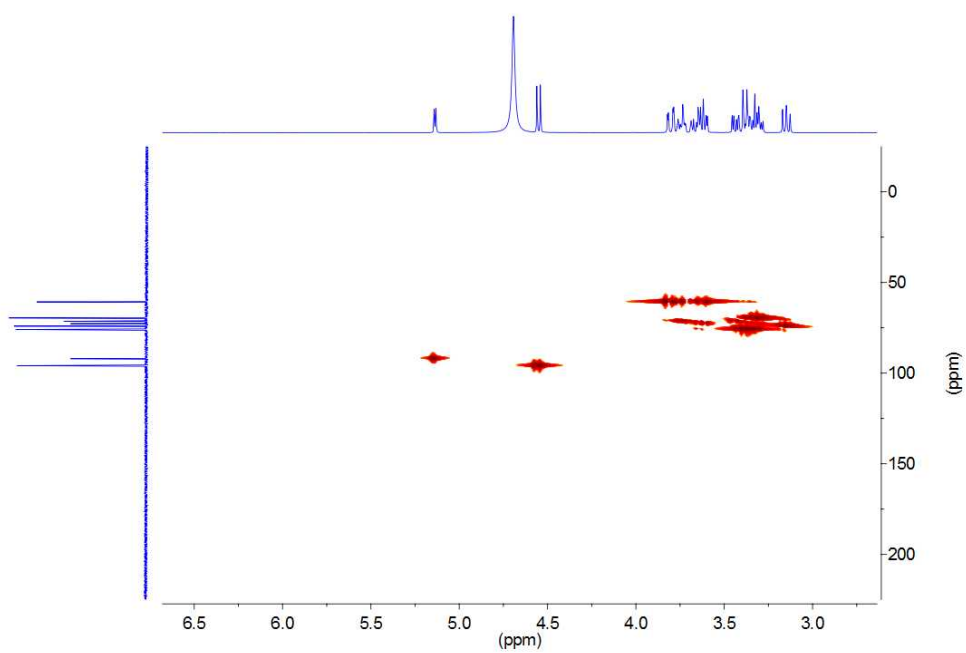


Figure S15. HMQC spectrum of glucose in D₂O.

9. TGA measurements

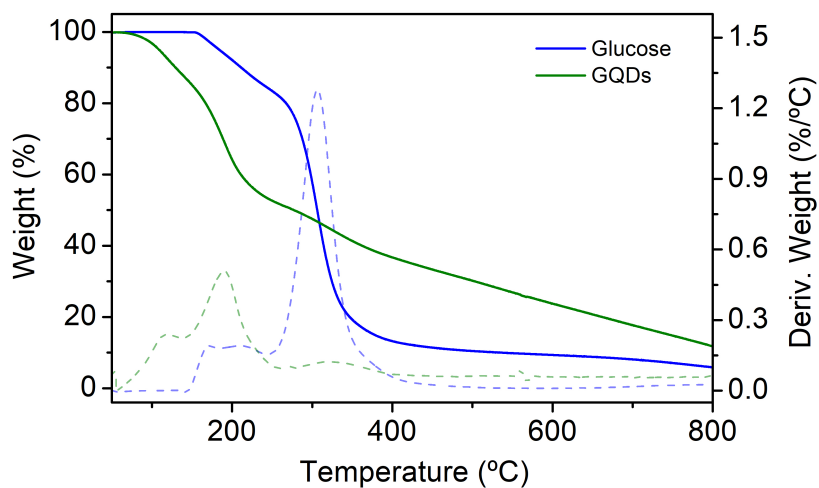


Figure S16. TGA of glucose, GQDs and their derivatives (dash lines). All the experiments were under N_2 , $10\text{ }^\circ\text{C min}^{-1}$.

The thermal degradation of GQDs in air exhibited different slope profile compared to the starting material, glucose (**Fig. S16**), especially in the final step of the decomposition, where two evident weight losses appeared. The weight loss from 370 °C was not observed for glucose and the weight loss from 470 °C exhibited higher intensity than for glucose. These losses reconfirm the presence of a GQD core without functional groups, that was more resistant to thermal degradation and burned completely once 600 °C was reached. Similar behaviors have been seen in other graphene nanomaterials such as graphene oxide.

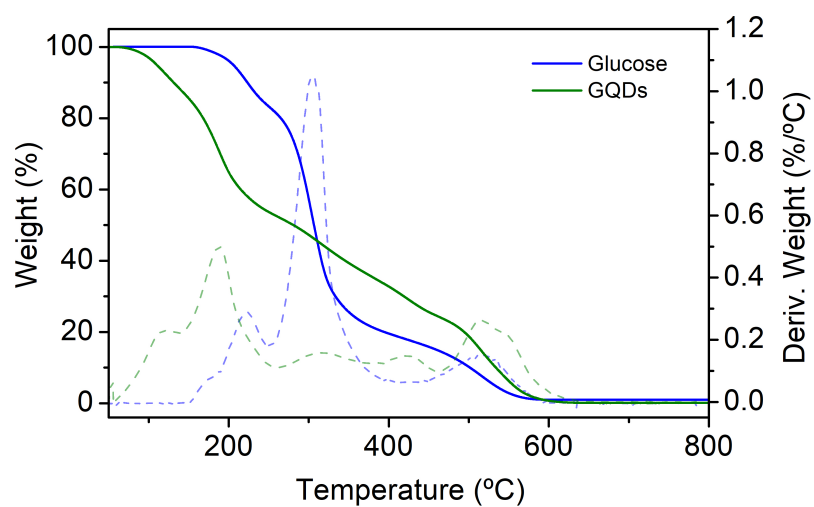


Figure S17. TGA of glucose (blue), GQDs (green) and their derivatives (dash lines). All the experiments were under air, $10\text{ }^{\circ}\text{C min}^{-1}$.

10. Raman measurements

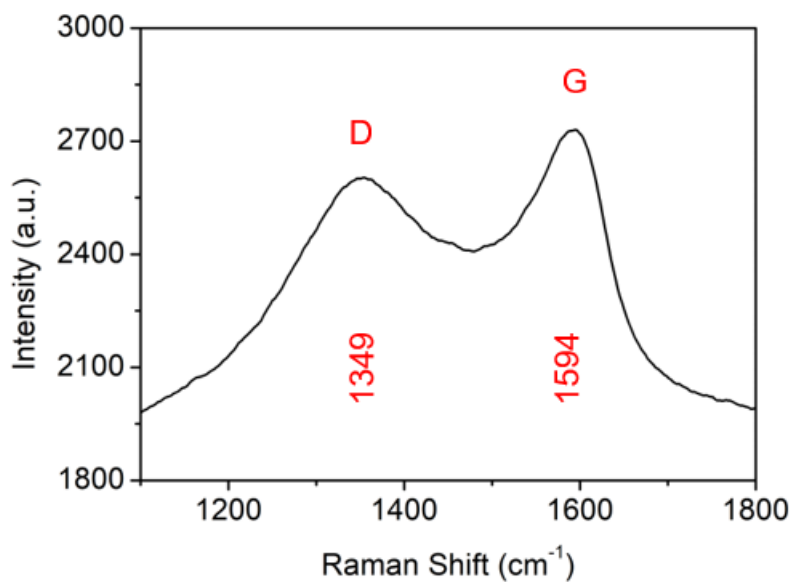


Figure S18. Raman spectrum of GQDs.

11. XRD measurements

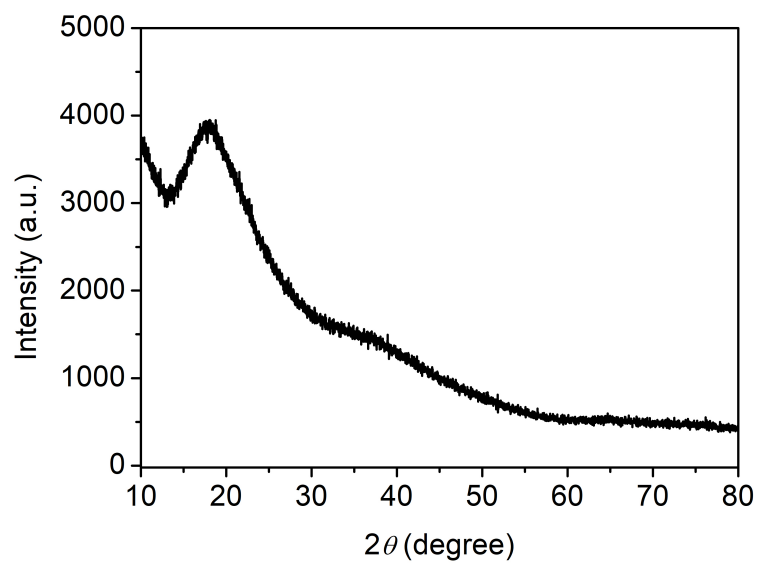


Figure S19. XRD pattern of GQDs.

12. Fluorescence measurements

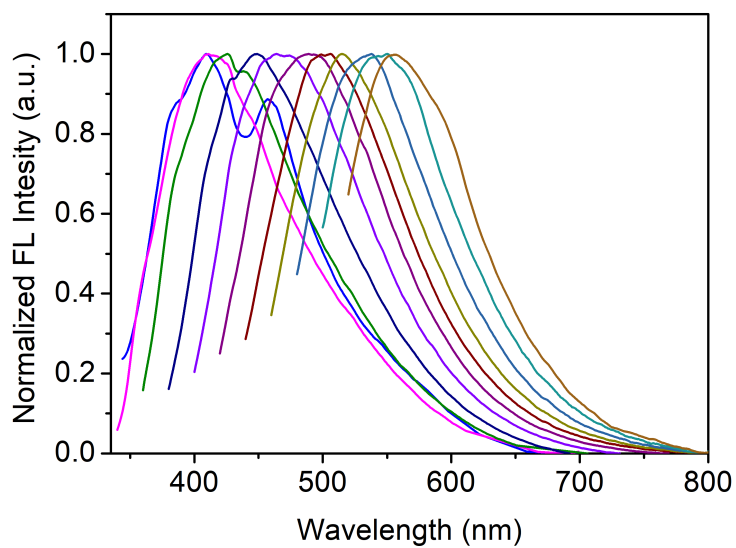


Figure S20. Normalized fluorescence spectra of GQDs in H₂O at different excitation wavelengths.

GQDs exhibited different maximum PL peaks after dissolving in various solvents (Figure S21). For instance, the maximum λ_{em} with solvents based on OH was λ_{em} 449 nm for MeOH and λ_{em} 445 nm for EtOH instead of λ_{em} 446 nm in water (*i.e.*, using λ_{ex} 360 nm). It can be seen that the dots contain many functional groups such as -OH, -NH₂, -COOH (Figure 3a), which can form strong hydrogen bonds with OH solvents (polar protic solvents). On the other hand, dipole-dipole interactions play a role in PL shifts λ_{em} 443 nm for acetone and λ_{em} 450 nm for DMSO (polar aprotic solvents). These observations manifest the solvent-dependent emission feature of our dots.

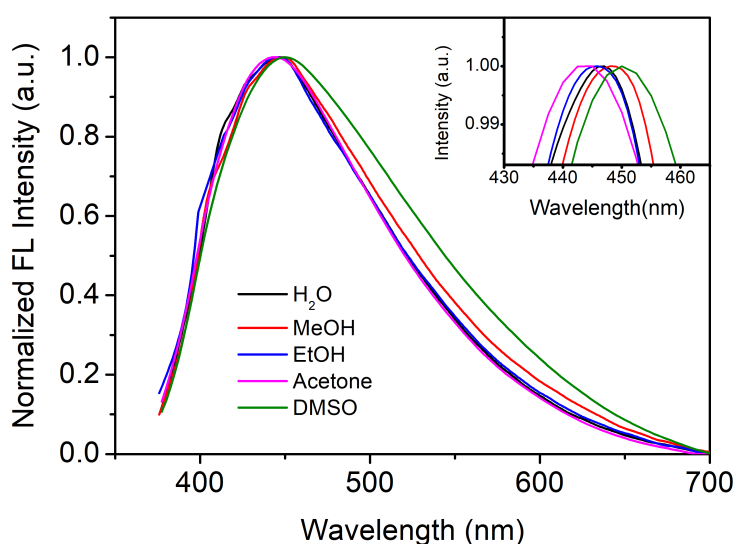


Figure S21. Normalized fluorescence spectra of GQDs in different solvents at λ_{ex} 360 nm. All spectra were recorded at room temperature.

13. Cell stability

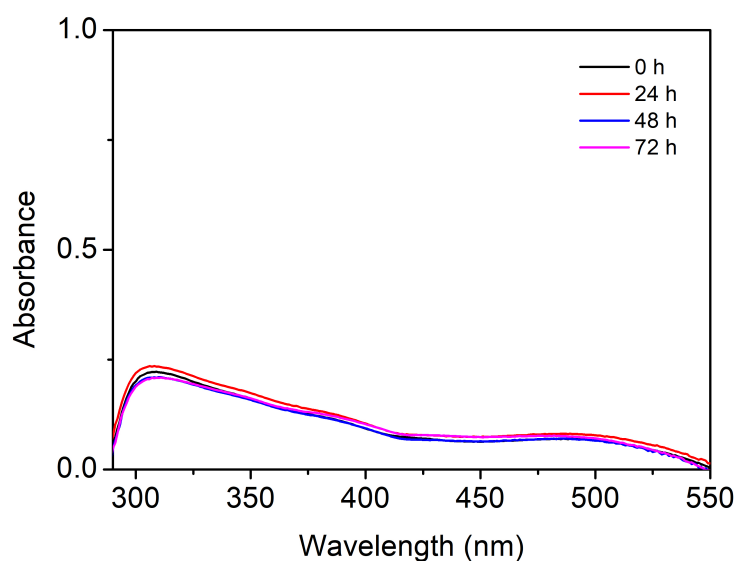


Figure S22. UV-Vis spectra of GQDs incubated in complete DMEM medium for 0 h, 24 h, 48 h and 72 h at 37 °C and 5% CO₂ in a humidified atmosphere.

14. Cell viability

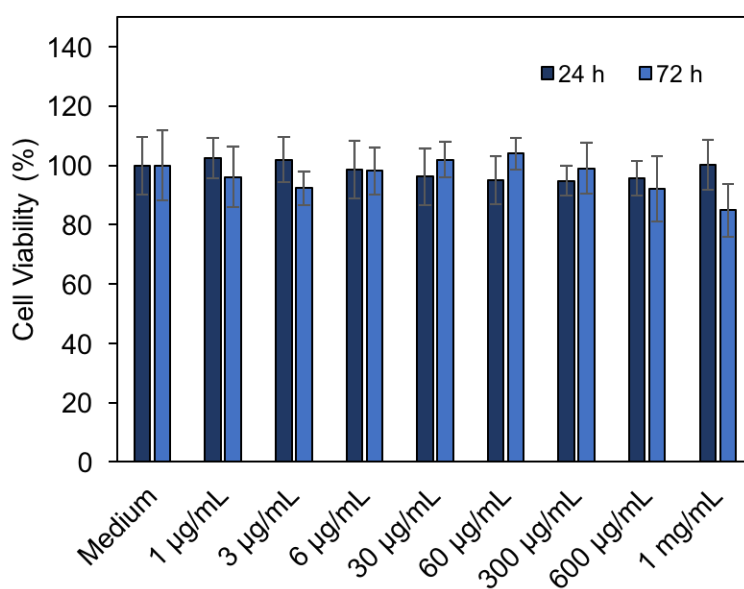


Figure S23. Cell viability assay with human vascular smooth muscle VSMC cells treated with different concentrations of GQDs in culture medium. Data are expressed as mean \pm SD

(n=3).

15. Confocal laser scanning microscope control images

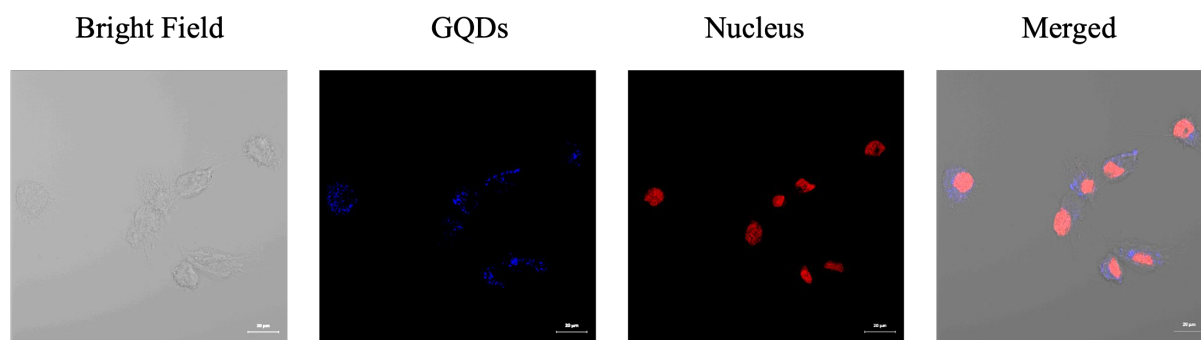


Figure S24. Cellular co-localization imaging of VSMC cells labeled with GQDs and DRAQ5 (nuclear stain). The images are shown in bright and fluorescence fields and their corresponding overlay. Scale bar 20 µm.

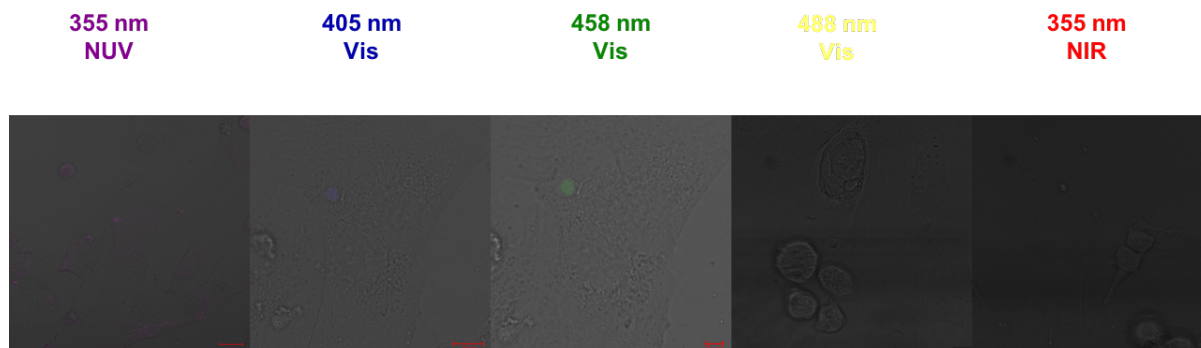


Figure S25. Control images of human vascular smooth muscle VSMC cells obtained by a confocal laser scanning microscope. Corresponding images under bright and fluorescence overlay fields.

16. References

- 1 S. Sarkar, D. Gandla, Y. Venkatesh, P. R. Bangal, S. Ghosh, Y. Yang and S. Misra, Graphene quantum dots from graphite by liquid exfoliation showing excitation-independent emission, fluorescence upconversion and delayed fluorescence, *Phys. Chem. Chem. Phys.*, 2016, **18**, 21278–21287.
- 2 W. Lu, Y. Li, R. Li, S. Shuang, C. Dong and Z. Cai, Facile Synthesis of N-Doped Carbon Dots as a New Matrix for Detection of Hydroxy-Polycyclic Aromatic Hydrocarbons by Negative-Ion Matrix-Assisted Laser Desorption/Ionization Time-of-Flight Mass Spectrometry, *ACS Appl. Mater. Interfaces*, 2016, **8**, 12976–12984.
- 3 Z. Rao, F. Geng, Y. Zhou, D. Cao and Y. Kang, N-doped graphene quantum dots as a novel highly-efficient matrix for the analysis of perfluoroalkyl sulfonates and other small molecules by MALDI-TOF MS, *Anal. Methods*, 2017, **9**, 2014–2020.
- 4 P. Kaiser, E.; Colescot, R.; Bossing, C.; Cook, Color Test for Detection of Free Terminal Amino Groups in the Solid-Phase Synthesis of Peptides, *Anal. Biochem.*, 1970, **34**, 595–598.